Water Resources Research

RESEARCH ARTICLE
10.1029/2019WR024983

Reactivation of Floodplains in River Restorations: Long-Term Implications on the Mobility of Floodplain Sediment Deposits

A.-L. Maaß[1] and H. Schüttrumpf[1]

[1]Insitute of Hydraulic Engineering and Water Resources Management, RWTH Aachen University, Aachen, Germany

Key Points:
- A Delft3D-model was used to evaluate the changes in the floodplain sediment deposition based on river restoration scenarios
- The goal is to increase the connectivity between the channel and floodplains by lowering the floodplain or raising the riverbed elevation
- Both river restoration scenarios lead to an increase in the fine sediment deposition on the floodplains

Correspondence to:
A.-L. Maaß,
maass@iww.rwth-aachen.de

Citation:
Maaß, A.-L., & Schüttrumpf, H. (2019). Reactivation of Floodplains in River Restorations: Long-Term Implications on the Mobility of Floodplain Sediment Deposits. *Water Resources Research*, *55*, 8178–8196. https://doi.org/10.1029/2019WR024983

Received 15 FEB 2019
Accepted 11 SEP 2019
Accepted article online 14 SEP 2019
Published online 23 OCT 2019

Abstract Nowadays, national and international requirements and laws emphasize the "natural" development of river-floodplain systems. One goal is to increase the connectivity between the river and its floodplains and thus reactivate floodplains as flooding areas, which potentially increases the mobility of fine sediments. The objective of this study is to analyze the long-term effects of reactivated floodplains on the mobility of floodplain deposits of small rivers based on two river restoration scenarios: elevating the riverbed or lowering the floodplains. Past channel fixation and degradation as well as the subsequent increase in the floodplain elevation led to the decoupling of the channel and floodplain morphodynamics associated with the reduction of the habitat connectivity. Here, the floodplain sedimentation rates were determined using a numerical model based on the Delft3D software. The novelty of these numerical investigations is the morphological long-term analysis over timescales of decades, which is not comparable to other short-term hydrodynamic and morphodynamic studies for small meandering lowland rivers. The results of 11 river restoration scenarios show that lowering the floodplain and raising the riverbed elevation both lead to an increase in the fine sediment deposition on the floodplain. However, lowering the floodplain elevation is generally more effective. Based on the numerical model results and the assumption of a fixed river channel, only anthropogenic activity might have increased the amount of fine sediments deposited on floodplains and has accelerated the decoupling of the floodplains from the riverbed in the past centuries.

1. Introduction

Many riverbeds incise several meters below their adjacent floodplains (Ghoshal et al., 2010; Scheffers et al., 2015; Surian et al., 2009; Surian & Rinaldi, 2003). In some cases, such an incision of the riverbed was constructed to reduce the flood risk and simultaneously increase the drainage of floodplains to increase the agricultural production (Kern, 1998). More often, incision of the riverbed develops unnoticed over decades in our river systems, for example, due to the construction and removal of transverse structures such as water mills (Buchty-Lemke & Lehmkuhl, 2018; Maaß & Schüttrumpf, 2019), river straightening (Frings et al., 2009), or anthropogenically increased discharges such as the input of mine, urban drainage, or industrial waters (Bizzi et al., 2015). Incised rivers have decreased water levels especially during low and mean flow conditions, and floodplain inundation suddenly occurs after heavy rainfall or snowmelt events. In Germany, only 10–30% of the original floodplains are still available as flooding areas (Brunotte et al., 2009; Ehlert & Neukirchen, 2012).

Many studies focused on the sedimentation processes on floodplains driven by hydrodynamics using event-based field measurements (e.g., Lambert & Walling, 1987, or Asselman & Middelkoop, 1995), numerical modeling approaches (e.g., Middelkoop & van der Perk, 1998; Narinesingh et al., 2010; Lauer & Parker, 2008a; Rudorff et al., 2018), or a combination of both to verify the results. For example, Middelkoop and van der Perk (1998) simulated the floodplain sediment deposition over river reaches with lengths of several kilometers using a geographic information system-based mathematical model and concluded that the model can be used to predict sediment deposition patterns, which are the results of the complex interaction among river discharge and sediment concentration, floodplain topography, and the resulting water flow patterns at various discharge levels. The numerical model results were compared with the sediment deposition patterns observed after the occurrence of a major flood event in the lower Rhine River in the Netherlands (Middelkoop & van der Perk, 1998).

At the same time, Narinesingh et al. (2010) simulated the floodplain sedimentation along extended river reaches with a series of alternating floodplains on both sides of the main channel and verified the approach using suspended load data obtained during flood events in the Ijssel River in the Netherlands. The numerical model of Narinesingh et al. (2010) can be used as a first approximation to estimate the quantity of the suspended load deposited on floodplains along extended river reaches during floods.

Today, 20 years after these studies, the analysis of floodplain sedimentation processes is still the main objective of morphological studies and river restoration interventions. For example, Fassoni-Andrade and Dias de Paiva (2019) first analyzed the sediment dynamics in large lakes and rivers of the central Amazon considering different water types (white, clear, and black water) using remote sensing images. With respect to today's river restoration interventions, national and international requirements and laws, for example, the EU Water Framework Directive or the "Room for the River" program, emphasize the "natural" development of river-floodplain systems. One goal is to increase the interconnection between rivers and their floodplains. River restorations include different interventions to counteract or eliminate the disconnection of the river from its floodplains. Generally, the deposition of fine sediment on floodplains is a natural process, whereas the disconnection of a river channel from its floodplains, for example, by an anthropogenically incised riverbed, is considered to be a negative morphodynamic change (Kern, 1998). Restorations encompass the removal of river bank or bed fixings, opening of channelized river parts, restoration of natural meander belts and cross-sectional profiles, increase in the riverbed elevation, dredging of floodplains, or flattening of river banks. For example, van Denderen et al. (2018) analyzed the mechanisms that influence the morphodynamic changes of side channels as a common intervention applied to increase the river's conveyance capacity and its ecological value in terms of river restorations in Europe and North America. Van Denderen et al. (2018) used a one-dimensional bifurcation model to predict the development of side channel systems and the associated timescale for a range of conditions and generalized them using stability diagrams including the most important model parameters. They showed, inter alia, that bank erosion hardly affects the equilibrium state but causes the side channel development over longer timescales depending on the bank erodibility (van Denderen et al., 2018). They concluded that the mechanisms in sand and gravel bed rivers are quite similar and that their results can therefore be used to assess the development and corresponding timescales of various side channel designs (van Denderen et al., 2018). Generally, restoration interventions should be sustainable, consider river-dependent hydrological and morphological characteristics, and lead to dynamic sediment transport processes.

In old-industrial areas, in which a lot of fine sediment is deposited on the floodplains and the riverbed has deeply incised, river restorations may lead to an extensive reconnection and remobilization of fine sediment. For example, a restoration intervention in the Ruhr River (219.3 km long with a catchment size of 4,485 km^2) was finished in 2013 CE, which included the widespread excavation of fine sediment deposited on the floodplains and the creation of additional retention areas. A restoration in the Möhne River (65.1 km long with a catchment size of 469 km^2), a tributary of the Ruhr River, was finished in 2008 CE. The main goals of the restoration were to remove the deep incision of the river and reduce the river bank heights. The cross-sectional area of the Möhne River was increased over a length of 700 m to generate variable and dynamic flow and habitat conditions.

The objective of this study is to analyze the effects of reactivated floodplains on the availability and mobility of floodplain deposits of small rivers. A numerical model based on the Delft3D software was used to analyze the long-term response of river morphodynamics due to reactivated floodplains. Two reactivation scenarios were considered: (1) increase in the riverbed elevation and (2) lowering of the floodplains. The schematized 2-D-numerical model represents small lowland rivers (river width <20 m) with wide floodplains (floodplain width ~150 m each side) deeply incised (river bank heights ~1–3 m). The numerical model is based on the topography and bathymetry of an 11-km reach of the Wurm River (Lower Rhine Embayment, Germany).

The outline of the paper is as follows: First, the characteristics of the Wurm River are described. Subsequently, the numerical model setup using the software Delft3D and the field measurement concept for the determination of the input data for the numerical model are described. Finally, the model results and future development focusing on fine sediment deposits on floodplains are presented and discussed. The conclusions are provided in the last section.

2. Materials and Methods

2.1. Study Site

The Wurm River flowing through the Lower Rhine Embayment has a catchment size of 356 km^2 and a length of 57.9 km (MULNV NRW, 2008). The channelization of the headwater tributaries underneath the city of Aachen leads to a significant reduction in the sediment load. In 2006 CE, approximately 2,500 m^3 sand was trapped in subsurface sand traps (personal communication in November 2016: Wasserverband Eifel Rur). The mean annual discharge is 3 m^3/s, and the mean flood discharge, which approximately equals the bankfull discharge, is 25 m^3/s (LANUV, 2004).

The Wurm River is characterized as a gravel bed river; however, fine sediment (clay, silt, and fine sand) is predominantly transported as suspended load. Downstream of the wastewater treatment plant Aachen-Soers, the Wurm River runs as a free meandering river toward the Dutch-German border. The Wurm River flows through an 11-km-long valley, which is rich in structure, and meanders over floodplains that are several hundred meters wide. The hillsides are partly forested (Fischer, 2000).

Figure 1 shows an overview of the upper part of the Wurm River from the source in the forest of Aachen to the city of Herzogenrath. The main anthropogenic impacts of the last 200 years on the Wurm River include the presence of a minimum of 60 water mills (Vogt, 1998), its location in the former underground coal mining area of Aachen, and channelization of the upper part of the Wurm River underneath the city of Aachen. The riverbed of the Wurm River is incised because of these anthropogenic effects, that is, due to the removal of the chain of water mills (Buchty-Lemke & Lehmkuhl, 2018; Maaß & Schüttrumpf, 2019) as well as the increased water discharge because of the inflow of purified wastewater (LANUV, 2004). Figure 1 shows the location of two turbidity sensors, which were installed in the Wurm River to determine the transport of suspended sediment.

2.2. Suspended Sediment Sampling

Data about the suspended sediment transport in the Wurm River obtained during different discharge events are not available. To collect such data, a measurement campaign consisting of two turbidity sensors, which continuously measure the turbidity in intervals of 5 to 10 min, and suspended sediment samples, which were taken from different locations of the Wurm River, was performed. The measurement campaign started in November 2016 CE and continued for a period of 2 years.

Following the principles of light absorption and scattering, turbidity (in nephelometric turbidity units, NTU) is defined as an optical property of a suspension that causes light to be scattered and absorbed rather than transmitted through suspension (Gippel, 1989). Turbidity in the water phase is caused by suspended particles such as clay, silt, organic, inorganic, or soluble colored organic substrate, plankton, and other microscopic organisms (Gippel, 1989, 1995; Habersack et al., 2008; Marquis, 2005). The particle shape has only a second-order effect on the turbidity (Davies-Colley & Smith, 2001). Optical backscattering sensors can be used as surrogates for the high-frequency determination of suspended sediment concentrations (SSCs) in rivers (Hoffmann et al., 2017; Schoelhammer & Scott, 2003). A measurement device (MPS-Qualilog 8, SEBA Hydrometrie & Co.KG) was used, which adopts optical backscatter technology to measure the turbidity. The turbidity sensor measures the unsolved suspended particles in the water phase. The scattered light of the turbidity particles is measured at an angle of 90°. Davies-Colley and Smith (2001) stated that only 1.5% of the light in natural river systems is scattered at an angle greater than 90°. With our measurement equipment, the turbidity between 0 and 1,000 NTU can be measured with a resolution of 0.01 NTU. The accuracy of the measurement device is $\pm$0.3 NTU for turbidity values <10 NTU and $\pm$3% for turbidity values >10 NTU. The device can be used at temperatures between 0 and 50 °C. A wiper in front of the measuring window cleans the sensor before each measurement. One turbidity sensor was installed at the start of the nearly natural part downstream of the wastewater treatment plant Aachen-Soers. The second turbidity sensor was installed at the end of the nearly natural river section, at the gauging station Herzogenrath. The locations of the measurement devices are shown in Figure 1.

The SSCs were determined by taking two 1.0-L water samples at each measurement location. During the gravimetric analysis, the water samples were filtered, dried in a drying oven at 105 °C for 48 hr, and weighted (with an accuracy of 0.1 mg). The SSC of these samples was determined using a smooth glass fiber filter (Macherey-Nagel, grade MN GF-6) without binder with a weight of 70 g/m^2, thickness of 0.35 mm,

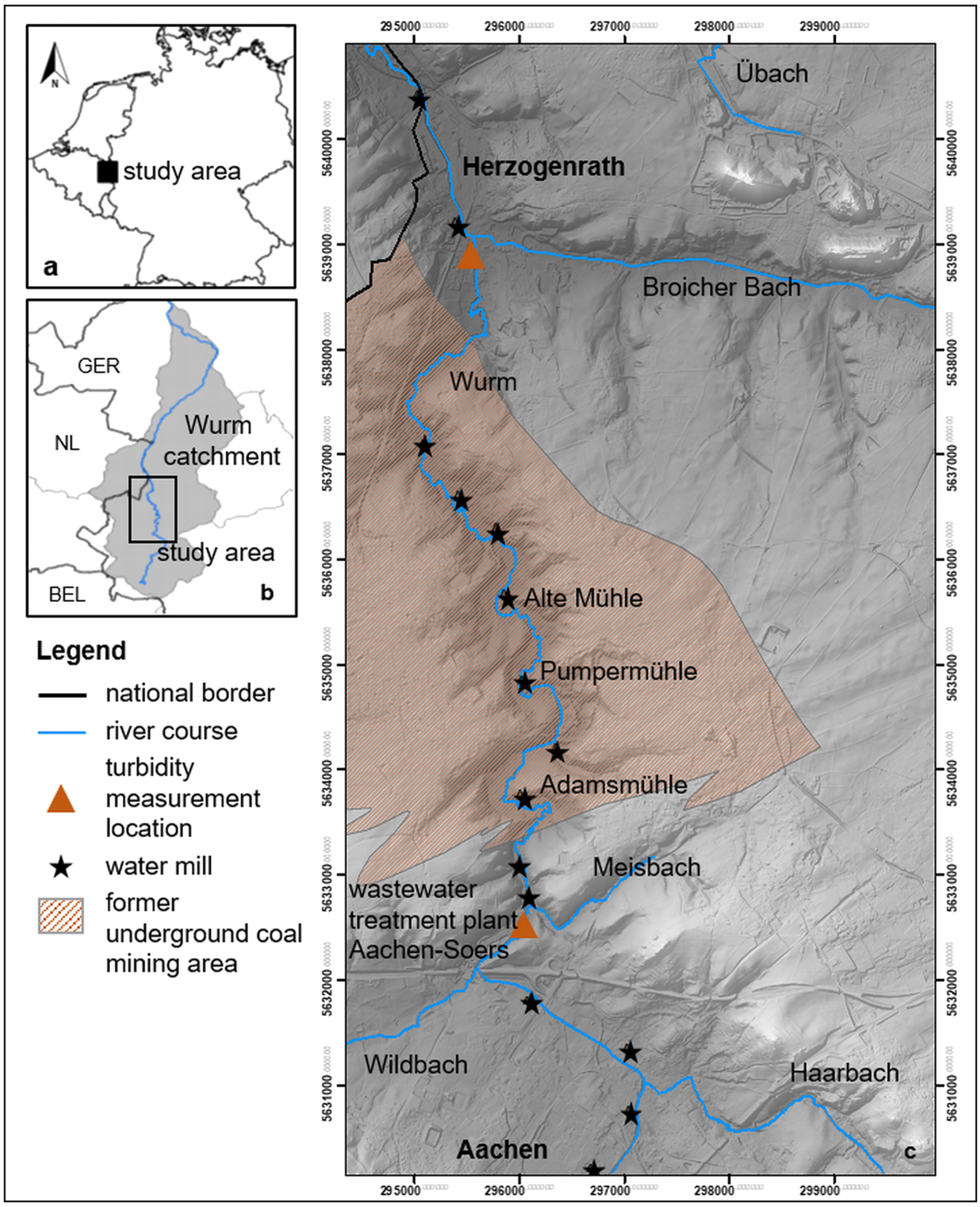

Figure 1. (a) Map of Germany and surrounding states, (b) Catchment of the Wurm River, and (c) study area of the Wurm River between the wastewater treatment plant Aachen-Soers and the city of Herzogenrath.

filtration speed of 12 s, average retention capacity of 0.6 μm, and migration distance of 140 mm per 10 min. Suspended sediment samples were collected monthly and, in addition, during flood events. Only 1-point sample was taken close to the turbidity sensor in the Wurm River because a high variability of the SSC in the vertical and horizontal directions of the cross-sectional profile was not expected. It is assumed that the SSC near the turbidity sensor equals the average SSC of the cross section.

Provided that most of the suspended sediment is fine grained (<2 mm) and that the grain size distribution is always the same, there is a good relationship between the turbidity and SSC (Buchanan & Schoellhamer, 1995; Christensen et al., 2000; Gilvear & Petts, 1985; Lewis, 1996; Lietz & Debiak, 2005; Rasmussen et al., 2005; Uhrich & Bragg, 2003; Walling, 1977). The sediment transported in suspension during the

measurement campaign in the Wurm River was always fine grained, and its composition insignificantly changes, even during flood events.

A continuous time series of SSCs can be obtained from turbidity values using quadratic regression analysis (Rasmussen et al., 2005). First, the recorded turbidity data sets were validated (checked for implausible values such as negative and duplicate values and outliers). A data point was marked as outlier when the measured value was twice as high as the prior or subsequently measured values (Habersack et al., 2005). Second, the SSC data were also checked for implausible values. The two parameters were then correlated with each other using quadratic regression analysis. The suspended sediment load (SSL) was determined by multiplying the SSC (g/m^3) with the prevalent discharge (m^3/s) and time (s) of that discharge.

2.3. Long-Term 2-D Modeling Using Delft3D

The long-term effects of reactivated floodplains on fine sediment deposits were investigated using the software Delft3D-Flow in 2-D (depth-averaged) mode. In the depth-averaged mode, the velocity distribution is averaged over the depth, the vertical resolutions of the velocities and pressures are neglected, and turbulent eddies are averaged using the Navier-Stokes equations (for further details, see Lesser, 2009, and Lesser et al., 2004).

A numerical model was used for the scenario analysis to determine the long-term effects of the mobility of floodplain sediment deposits. The model is based on the characteristics of the 11-km section of the Wurm River between the wastewater treatment plant Aachen-Soers and the city of Herzogenrath (see Figures 1 and 2). The total number of grid cells is 98,952, and the average cell size of the entire model is 26.3 m^2. The main channel is represented by approximately four grid cells with average cell widths and lengths between 3 and 5 m. The curvilinear grid structure of the Delft3D software leads to problems in sharp bends. To avoid numerical instabilities, the course of the Wurm River was modified at several locations, and sharp meander bends were cut to obtain a straight river course. Based on these simplifications, the differences in the flow conditions between the numerical model and original Wurm River were completely neglected in this analysis. Generally, a reduced flow length leads to higher flow velocities, less floodplain inundation, and thus decreased sedimentation rates. This study focused on a scenario-based analysis of different river restoration interventions and not on the Wurm River. Therefore, the exact prediction of, for example, floodplain inundation areas and amounts of sediment deposition on floodplains is not of interest. The results of the different scenarios were compared with the reference case, and the course of the river was constant in all scenarios. The left part of Figure 2 shows the small differences in the river course between the numerical model and original Wurm River. The grid cells of the riverbed were constructed with high resolution, which does not impose any limitations on the floodplain dynamics. The sediment dynamics in the riverbed were not analyzed in detail.

The topography of the model is based on a digital elevation model (LiDAR DEM, spatial resolution of 1 m, height resolution of $\pm$0.2 m; Land, 2017). The current bathymetry is linearly interpolated between bathymetry cross sections with an average spacing of 100 m.

The boundary conditions correspond to those recently published by Maaß and Schüttrumpf (2018): a quasi-steady time-dependent inflow hydrograph at the upstream boundary (for a detailed description of this simulation management tool of Delft3D, see Yossef et al., 2008) and discharge-water depth relation at the downstream boundary. The hydrologic time series were based on discharge measurements at the gauging station in Herzogenrath performed between 1969 CE and 2016 CE. The discharge ranges from 0.13 to 44.30 m^3/s. In this study, five quasi-steady discharge steps between 10 and 50 m^3/s were defined.

All measurement results were used as a basis for the quasi-steady morphological modeling approach that captures characteristic flow situations such as the average flow, and bankfull conditions, and overbank flow. Each numerical modeling scenario considers a total morphological duration of 10 years.

The suspended sediment transported in the model is equal to 24.5 μm (silt), which represents the median diameter (D_{50}) of sediment cores taken from the floodplains of the Wurm River and is similar to the averaged D_{50} of sediment samples taken from the Wurm River during the turbidity measurement campaign. The transport of cohesive sediment was modeled using the Partheniades-Krone equation (Partheniades, 1965). The sediment input was based on the results of the quadratic regression analysis of the turbidity and SSC measurements from November 2016 CE and November 2018 CE (see section 3.1). In addition, one major

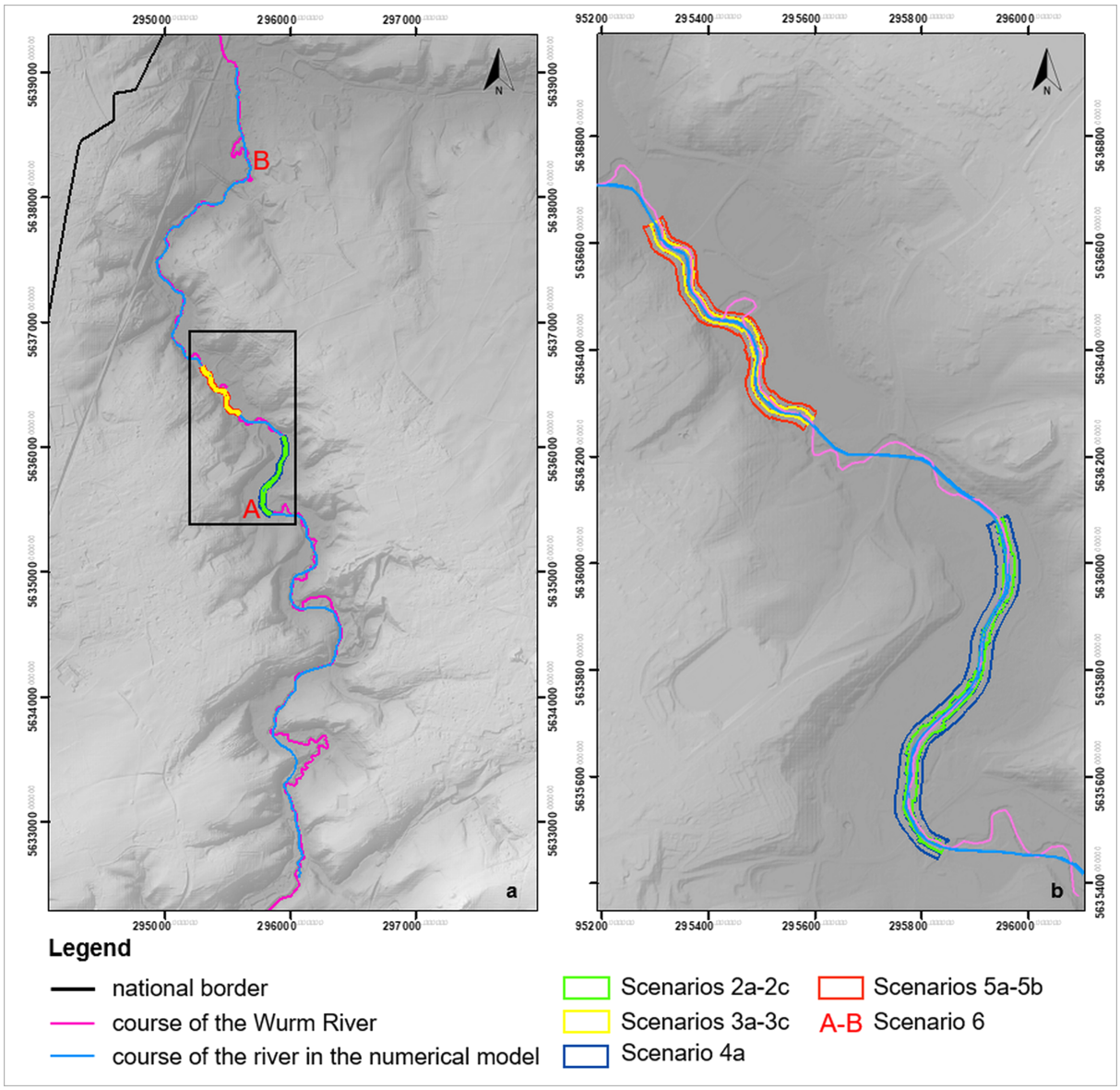

Figure 2. Locations of the numerical model scenarios.

assumption of the numerical model is that the entire riverbed consists of gravel with a D_{50} value of 33 mm and that the bed-load transport is negligible, even under bankfull and overbank discharge conditions. Local processes, such as riverbank erosion, vegetation, or cohesive forces (e.g., Kleinhans et al., 2018; Schuurman et al., 2016, 2018), are often simulated using a single-simplified numerical model or separated numerical models. Both were not applied here. The results of the assessment of the model quality and assumptions are provided in section 4.3.

Generally, the backgrounds of the hydrodynamic and morphodynamic calibrations are the same as those recently published by Maaß and Schüttrumpf (2018). The critical shear stresses for the erosion and sedimentation were determined using the two median grain sizes of the floodplains ($\tau_{c,ero,floodplain} = 12$ N/m^2; $\tau_{c,sed,floodplain} = 1{,}000$ N/m^2) and riverbed ($\tau_{c,ero,riverbed} = 45$ N/m^2; $\tau_{c,sed,riverbed} = 1$ N/m^2). In this study, a constant roughness value is used for the river and the floodplains. The water levels with a relative maximum deviation of −0.11%, correlation coefficient of 0.999, and Nash-Sutcliffe index of 0.96 (Nash & Sutcliffe, 1970) were reproduced with a Chézy coefficient of 31 m$^{1/2}$/s.

Table 1
Scenarios of River Restorations Focusing on the Reconnection of the Riverbed and the Floodplains

Scenario	Adjustment	Location	Height (m)	Length (km)	Width (m)
1	—	—	—	—	
2a	Increase	Straight, middle of the valley	+0.3	1	10–15 (entire riverbed)
2b	Increase	Straight, middle of the valley	+0.7	1	10–15 (entire riverbed)
2c	Increase	Straight, middle of the valley	+1.0	1	10–15 (entire riverbed)
3a	Increase	Meandering, close to the left valley flank	+0.3	1	10–15 (entire riverbed)
3b	Increase	Meandering, close to the left valley flank	+0.7	1	10–15 (entire riverbed)
3c	Increase	Meandering, close to the left valley flank	+1.0	1	10–15 (entire riverbed)
4a	Lowering	Straight, middle of the valley	−1.3	1	20 (each floodplain)
5a	Lowering	Meandering, close to the left valley flank	−1.3	1	20 (each floodplain)
5b	Lowering	Meandering, close to the left valley flank	−1 3	1	20 (each floodplain)
6	Increase	Entire modeling area	+0.7	7	10–15 (entire riverbed)

2.4. Scenarios

Two types of river restorations were considered in this study, which both are suitable to enhance the connectivity of riverbeds and their floodplains. Each scenario had a total morphological duration of 10 years.

First, the riverbed elevation was increased. The entire riverbed, including the elevated riverbed, consists of gravel with a D_{50} value of 33 mm. The sediment transported in suspension is silt with a D_{50} value of 24.5 μm. The increase in the riverbed elevation decreases the riverbank heights and increases the connection between the riverbed and floodplains.

Second, the floodplains were excavated, which also decreases the riverbank heights and increases the connection between the floodplains and riverbed. The riverbed consists of gravel with a D_{50} value of 33 mm, and the sediment transported in suspension is silt with a D_{50} value of 24.5 μm. The floodplain deposits were excavated and removed. The surface of the floodplain consists of silt with a D_{50} value of 24.5 μm. Table 1 summarizes all scenarios, and Figure 2 shows the scenario locations.

Currently, there are no river restorations planned in the study area of the Wurm River. Therefore, the different scenario locations were selected based on different topographical valley settings and the characteristics of the main river channel. Scenarios 2 and 4 were set in a straight part of the Wurm River in the middle of the valley. Scenarios 3 and 5 were set in a meandering part of the Wurm River closer to the valley flanks.

Scenario 1 represents the reference scenario. In all other scenarios, the elevations of the riverbed or floodplains of the model mesh were manually increased or decreased by a defined height in a defined area. In Scenarios 2a, 2b, and 2c, the riverbed elevation was partially increased by +0.3, +0.7, and +1.0 m, respectively, over a length of 1 km. In Scenarios 3a, 3b, and 3c, the riverbed elevation was partially increased by +0.3, +0.7, and +1.0 m, respectively, over a length of 1 km. In Scenario 4a, the floodplains were excavated by −1.3 m, with a width of 20 m on each floodplain side, over a length of 1 km. In Scenario 5a, the floodplains were excavated by −1.3 m, with a width of 20 m each floodplain side, over a length of 1 km. In Scenario 5b, the width of the floodplain to be lowered was increased to ~100 m. In Scenario 6, the riverbed elevation was increased by +0.7 m over almost the entire length of the model (~7 km).

3. Results

3.1. Regression Results

The turbidity data sets and SSCs measured between 14 November 2016 CE, and 2 November 2018 CE were analyzed (see Figure 3). The data show a large amount of scatter and hysteresis, which are not of interest due to the long-term approach of this study. The discharge during this period ranges from 0.10 to 37 m^3/s, with an average of 0.63 m^3/s, in Aachen-Soers and from 0.43 to 52 m^3/s, with an average of 1.64 m^3/s, at the gauging station in Herzogenrath (LANUV, 2018).

For the data from Aachen-Soers, quadratic regression was performed using 27 SSCs. Four of these 27 values were marked as implausible values. For the data from Herzogenrath, the quadratic regression was performed using 27 SSCs. Three of these 27 values were marked as implausible values. Based on the data sets, different forms of fitted curves were tested to relate the measured SSCs to the turbidity values. A polynomial

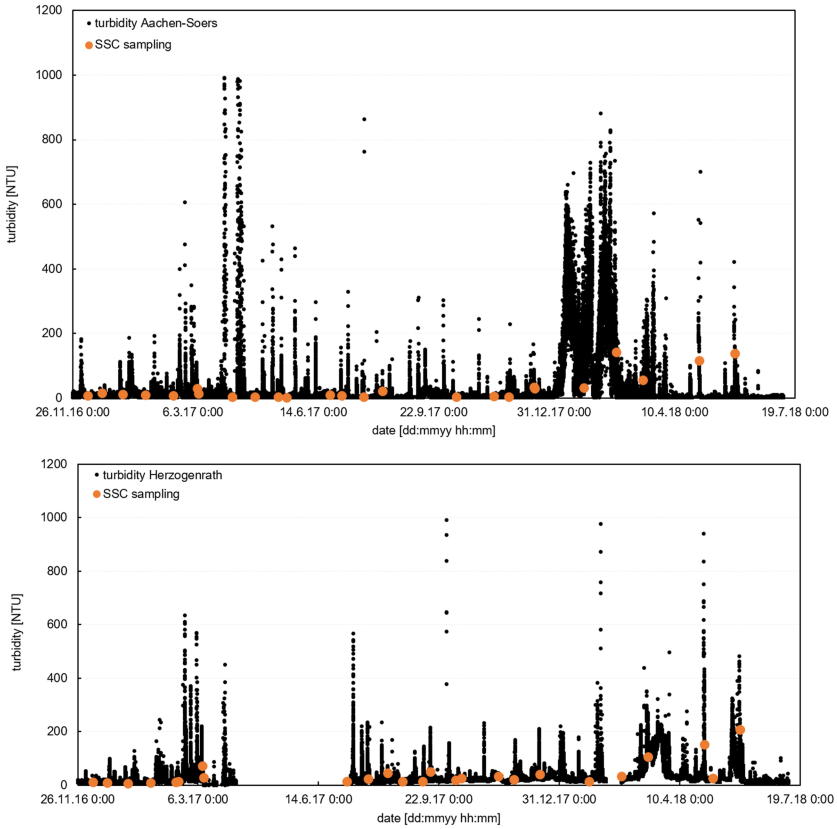

Figure 3. Turbidity data sets of the Wurm River in Aachen-Soers and in Herzogenrath between 2016 CE and 2018 CE. SSC = suspended sediment concentration.

regression equation was used, which best describes the relation between the turbidity and SSC at the two measurement locations, that is, in Aachen-Soers (see equation (1), coefficient of determination (R^2) of 0.80) and in Herzogenrath (see equation (2), coefficient of determination [R^2] of 0.94):

$$\mathrm{SSC} = 0.0036\mathrm{T}^2 + 0.7535\mathrm{T}, \tag{1}$$

$$\mathrm{SSC} = 0.0104\mathrm{T}^2 + 1.1938\mathrm{T}, \tag{2}$$

where SSC is the suspended sediment concentration in milligrams per liter and T is the turbidity in NTU, ranging from 0 to 1,000 NTU. Figure 4 shows the results of the polynomial regression for both measurement locations.

At the measurement locations in Aachen-Soers and Herzogenrath, a SSL of 21 and 43 tons per year was determined. Because of the small variability and organic content in the Wurm River, the data set was not separated into winter and summer periods. Therefore, only one SSL was calculated for the entire year. Note that two extreme flood events occurred in the Wurm River between November 2016 CE and November 2018 CE (with reoccurrence intervals of 50 and of 100 years), which led to a higher average annual SSL compared with other periods without such extreme events.

The SSC values determined using equations (1) and (2) for both measurement locations were related to the prevalent discharge and separated according to the discharge classes of the quasi-steady hydrograph. Table 2 shows the average SSC for each discharge class of the quasi-steady hydrograph.

Specific study site conditions of the Wurm River due to rainwater retention basins, flood control reservoirs, and sewer overflows were not included in the Delft3D model. In the numerical model, it was assumed that the sediment input generally increases with increasing discharge. Therefore, the sediment input of the Delft3D model is based on the results of the field measurements in Aachen-Soers (see Table 2) but was

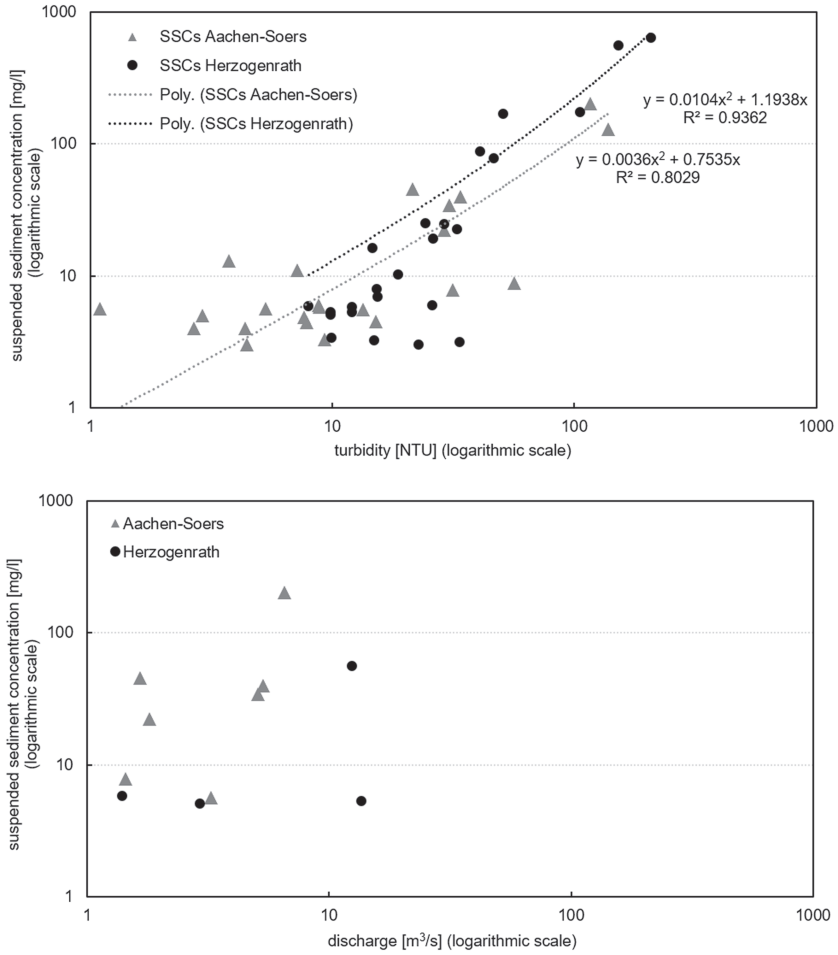

Figure 4. Turbidity against SSC values (upper part) as well as discharge against SSC values (lower part) measured in Aachen-Soers and Herzogenrath between November 2016 CE and November 2018 CE. SSC = suspended sediment concentration.

adjusted and extrapolated to reflect an increasing sediment input with increasing water discharge. Table 2 also shows the sediment input of the Delft3D model based on the field measurement results for the Wurm River. All scenario simulations were performed using these sediment inputs.

3.2. Delft3D Modeling Results

The average floodplain sedimentation was calculated by summing the amount of floodplain sedimentation in all grid cells of all discharge classes and dividing it by the amount of grid cells in which floodplain

Table 2
Average SSC in Kilograms per Cubic Meter for Each Discharge Class in the Wurm River in Aachen-Soers and in Herzogenrath Measured Between November 2016 CE and November 2018 CE and Used in the Delft3D Model as Sediment Input Data at the Upstream Boundary of the Model

Discharge class (m^3/s)	SSC (kg/m^3) in Aachen-Soers	SSC (kg/m^3) in Herzogenrath	SSC (kg/m^3) in Delft3D
10	0.12	0.57	0.12
20	0.34	1.88	0.34
30	0.09	1.92	0.65
40	Not measured	1.94	1.02
50	Not measured	1.96	1.48

Note. SSC = suspended sediment concentration.

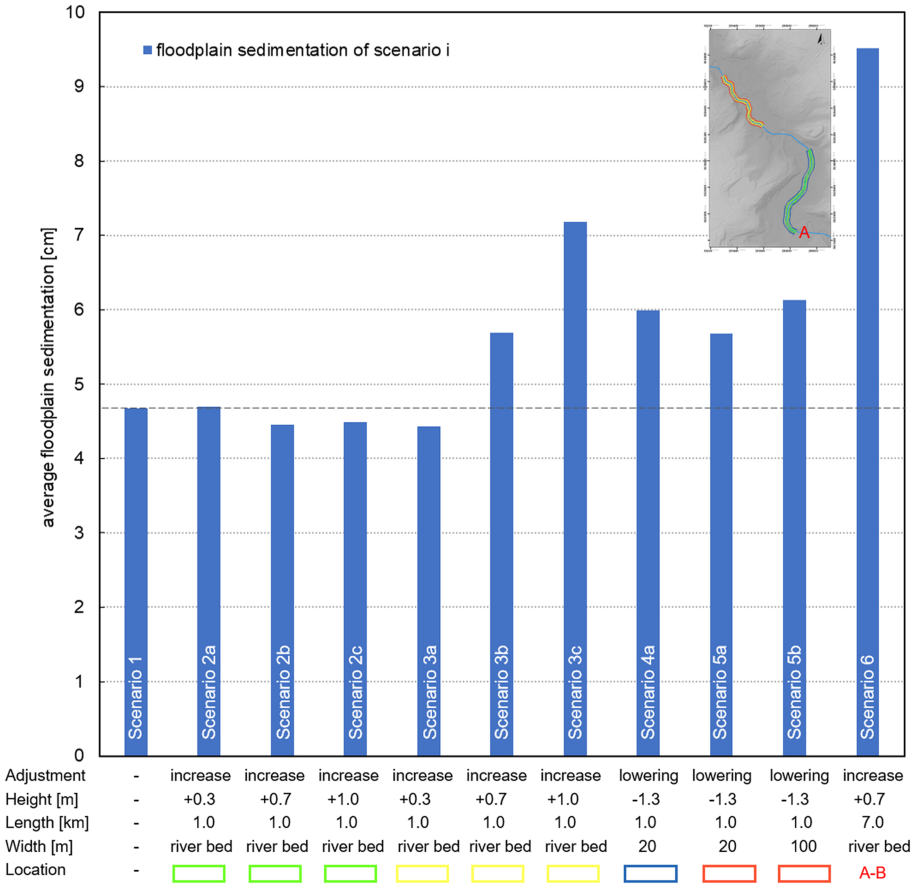

Figure 5. Average floodplain sedimentation of the entire model area of all scenarios.

sedimentation took place. Depositional and erosional processes close to the upstream and downstream boundaries of the model (~500 m) were neglected to avoid inaccuracies due to numerical boundary effects.

Figure 5 shows the average floodplain sedimentation of the entire model area for all scenarios. The average floodplain sedimentation of the reference Scenario 1 for the upcoming 10 years is 5 cm. Generally, the results of Scenario 2 show a decrease in average floodplain sedimentation in the entire model area compared with Scenario 1, whereas the results of Scenarios 3 to 6 show an increase in the average floodplain sedimentation in the entire model area compared with Scenario 1.

3.2.1. Effects of the Riverbed Elevation

The results for Scenarios 2a, 2b, and 2c show that the increase in the riverbed elevation results in less sediment deposition in the modeling area (see Figure 5). Because of the main assumption of the numerical model that the riverbed is fixed, scouring cannot be observed.

In contrast, the numerical model results for Scenarios 3b and 3c show that the larger the increase in the riverbed elevation, the larger the average floodplain sedimentation on the entire floodplain area. With respect to the impact of timing, Scenarios 3b and 3c change the floodplain inundation frequencies and activate floodplains at lower discharges. The increase in the riverbed elevation results in longer sediment settling times on the floodplains and therefore in more floodplain sedimentation. The average sedimentation of Scenario 3a (increase by +0.3 m) is >4 cm, which is less than the average sedimentation of ~6 cm of Scenario 3b (increase by +0.7 m) and ~7 cm of Scenario 3c (see Figure 5). The spatial configuration of the sediment deposition increases with increasing riverbed elevation until the flanks of the valleys, and therefore, the maximum extension of the floodplain inundation is reached.

In addition to the spatial distribution of the floodplain inundation, changes in the shear stress of the floodplains lead to changes in the floodplain deposition. Regarding the shear stress of the floodplains at the maximum discharge of the quasi-steady hydrograph ($Q = 50\ m^3/s$), the shear stress in the restoration area of

Scenario 2 equals ~2 N/m^2 and does not change with increasing riverbed elevation compared with the shear stress in the reference area of Scenario 1. In contrast, the increase in riverbed elevation of Scenarios 3b and 3c leads to an increase in the shear stress of the floodplains from ~2 to ~4 N/m^2.

The results of scenario 6 show the greatest changes in the floodplain sedimentation after the riverbed elevation was increased. In Scenario 6, the riverbed was increased over a length of ~7 km, that is, almost the entire length of the numerical model. Therefore, large floodplain areas are reactivated until the maximum extension of the floodplain inundation is reached. Additionally, the shear stress of the floodplains increases in almost over the entire modeling area from 2 N/m^2 (Scenario 1) to 4 N/m^2 (Scenario 6). The average floodplain sedimentation of the entire floodplain area of the numerical model (~9.5 cm) increases by almost 100% compared with the reference Scenario 1 (<5 cm; see Figure 5).

Generally, an increase in the riverbed elevation does not lead to floodplain inundation at lower discharges but to a greater inundation expansion during flood events, which increases the floodplain sedimentation. Figure 6 shows the water depths of Scenario 3b compared with the reference Scenario 1 at a discharge of 50 m^3/s (upper part of Figure 6) as an example for the spatial changes in the water depth due to an elevated riverbed. Generally, further changes in the depositional rates as a result of the hydrograph patterns are of secondary importance in such a long-term analysis and cannot be determined due to the quasi-steady hydrograph approach of the scenario analysis.

3.2.2. Effects of Floodplain Lowering

The floodplain area that is lowered in Scenario 5b is wider than that of Scenario 5a. The comparison between Scenarios 5a and 5b shows that the wider the lowered floodplain area (20 m in Scenario 5a compared with 100 m in Scenario 5b), the larger the average floodplain sedimentation in the entire floodplain area (~5.5 cm in Scenario 5a and >6 cm for Scenario 5b; see Figure 5). In this study, the shear stress of the floodplains increases in all scenarios in which the floodplain elevation was lowered, from 2 N/m^2 (reference scenario 1) to 4 N/m^2 (Scenarios 4a, 5a, and 5b).

Generally, lowering the floodplains leads to the inundation of terraces and floodplain areas at lower discharges compared with the reference Scenario 1. The lower part of Figure 6 shows the water depths of Scenario 4a compared with the reference Scenario 1 at a discharge of 10 m^3/s as example for the changes in water depth due to the lowering of floodplains.

3.2.3. Comparison of all Results

The results of Scenarios 2a–2c and 3a–3c) with increased riverbed elevations are contrary. In Scenario 2, the floodplain inundation frequencies do not change, and thus, the floodplains are not activated at lower discharges compared with reference Scenario 1. In Scenario 2, the flow paths and extension of floodplain inundation directly downstream of the restoration area change due to the increase in the riverbed elevation.

Figure 7 shows the average floodplain sedimentation related to the restoration area for all scenarios compared with the reference Scenario 1 to analyze the effects of the restoration related to upstream and downstream effects. In contrast to Figure 5, the average floodplain sedimentation is only determined for the restoration area in Figure 7 and not for the entire model area.

The comparison of the average floodplain sedimentation with the restoration area shows that the floodplain sedimentation in the restoration area does not increase with increasing riverbed elevation. The lower the increase in the riverbed elevation (Scenario 2a: +0.3 m; Scenario 2c: +1.0 m), the higher the average amount of floodplain sedimentation in the restoration area (Scenario 2a: 6 cm; Scenario 2c: 3 cm; see Figure 7). The average floodplain sedimentation of Scenario 3c (increase by 1.0 m) is smaller than the average floodplain sedimentation of Scenario 3b (increase by 0.7 m; see Figure 7).

The numerical model results of Scenario 2 show that an increase in the riverbed elevation does not lead to the effects desired for reactivated floodplains and an increase in the fine sediment deposits on the floodplains. In contrast, the lowering of the floodplains at this location (Scenario 4a) leads to a high increase of the floodplain sedimentation in the restoration area (Scenario 4a: 24 cm; Reference Scenario 1: ~7 cm; see Figure 7).

The average floodplain sedimentation in the restoration area of Scenario 5b (>6 cm) is smaller than that of Scenario 5a (~9 cm; see Figure 7). These effects are related to the different changes in the floodplain inundation of Scenarios 5a and 5b. An analysis of the floodplain inundation frequencies of Scenarios 5a and 5b shows that the lowering of Scenario 5b leads to higher floodplain inundation frequencies in the

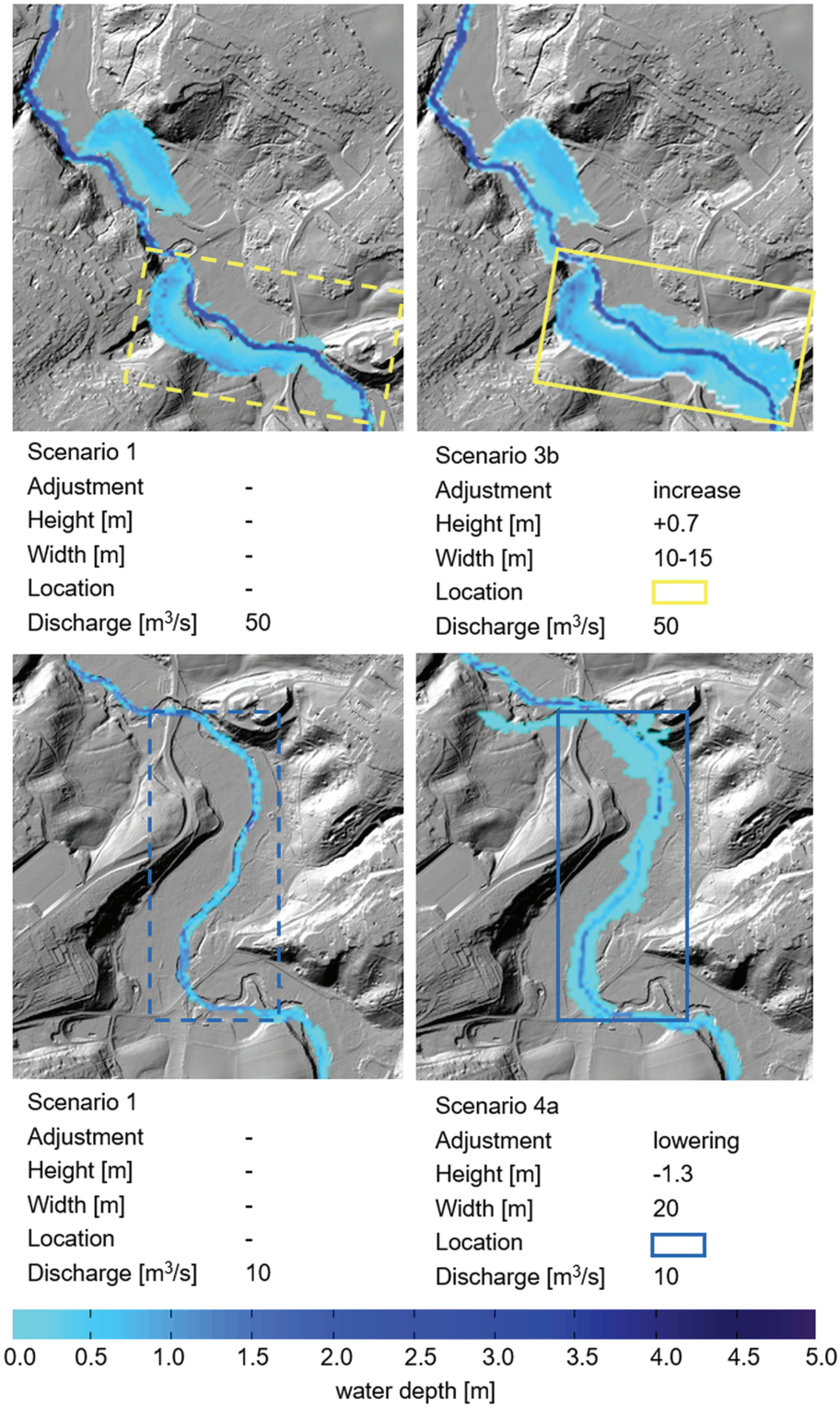

Figure 6. Comparison of the water depths of the reference Scenarios 1 and 3b at a discharge of 50 m^3/s (upper part) and Scenario 4a at a discharge of 10 m^3/s (lower part).

restoration area and downstream of the restoration area, which also increases floodplain sedimentation downstream of the restoration intervention. Scenario 5a only increases the floodplain inundation frequency in the restoration area.

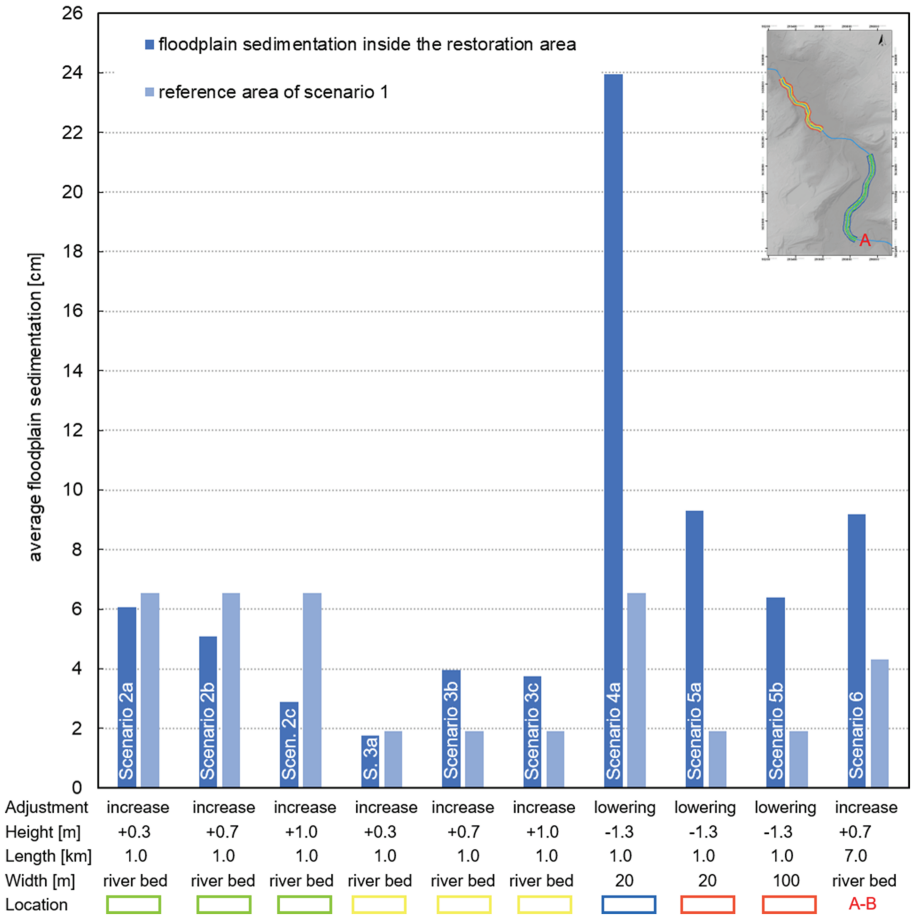

Figure 7. Average floodplain sedimentation inside the restoration area in comparison to the reference area of Scenario 1.

The increase in the floodplain sedimentation of Scenario 4 is greater than the increase in the floodplain sedimentation of Scenario 5, but Scenarios 3b and 3c lead to higher floodplain sedimentation than Scenarios 2a, 2b, and 2c (see Figures 5 and 7). Consequently, the results show that the local flow conditions become more important in case of an increase in the riverbed elevation than in case of a decrease in the floodplain elevation.

With respect to the relative influence of the valley confinement on the floodplain deposition, the results of the numerical scenarios show that an increase in the riverbed elevation does not increase the floodplain sedimentation, although Scenario 2 is set in a straight part of the Wurm River in the middle of both valley flanks. In contrast, Scenario 3 leads to an increase in the floodplain sedimentation on the right floodplain of the Wurm River. The position of the river close to the left valley flank increases the flow velocities and flow direction toward the right river bank. Therefore, the right floodplains are inundated earlier, and the river uses the additional floodplain area of ~125 m on the right floodplain.

The comparison of the average floodplain sedimentation of the entire floodplain area (see Figure 5) with the average floodplain sedimentation in the restoration area (see Figure 7) of Scenarios 4a, 4b, and 5 shows that the consequences of the lowering of the floodplains are predominantly remarkable in the restoration area. The difference (Scenario 4a: ~1 cm) between the average floodplain sedimentation of the entire floodplain area of Scenario 4a (~6 cm; see Figure 5) and that of the reference Scenario 1 (<5 cm; see Figure 5) is smaller than the difference between the average floodplain sedimentation in the restoration area (18 cm; Scenario 4a: 24 cm; Scenario 1: 6 cm; see Figure 7).

4. Discussion

4.1. River Management Strategies

Restoration interventions are always in an area of tension between securing flood protection, reestablishing natural discharge conditions, considering urban management and the protection of historical buildings, natural river development and maintenance, and public perception and acceptance (Berends et al., 2018). Wohl et al. (2015) stated that the challenges with respect to river restoration are based on the large gap between the knowledge of processes, such as sediment transport, and the ability to use that knowledge for predictions or measurements in river restorations.

Focusing on the location of a river restoration within river management strategies, the results of Scenarios 3 and 5 show that the reactivation of floodplains in a small, defined area has significant consequences for downstream areas because of the flow paths and floodplain inundation changes due to the reactivation of the floodplains. In both scenarios, the average floodplain sedimentation of the entire model increases compared with Reference Scenario 1 (see Figures 5 and 7). The results of Scenario 5 show that the increase in the floodplain sedimentation is not only related to the restoration area but also to the entire river system (see Figures 5 and 7). Overall, the transport of sediment in downstream direction also depends on the location of a river restoration. Generally, an increased trapping of sediment in an upstream area of a river leads to downstream depletion of sediment (unless bank erosion or other additional sediment inputs occur).

Based on the assumption of a fixed riverbed, the numerical model results do not show an increased remobilization of the sediments due to a greater degree in connectivity between the river channel and floodplains. In principle, erosion of the floodplain sediments is possible if the shear stress in the floodplains exceeds the critical shear stress of the floodplains specified during the model setup (12 N/m^2 in this study). The maximum prevalent shear stress required for the erosion of the floodplains for all scenarios is 8 N/m^2. Therefore, the critical shear stress is not exceeded during floodplain inundation, and the floodplain sediment deposits are not mobilized. Consequently, the results of all scenarios indicate that the deposition of fine sediment is the dominant transport process on the floodplains.

Additionally, the numerical model results show that an increase in the riverbed elevation and the excavation of floodplains result in an increase in the fine sediment deposits on the floodplains. The contrary results of Scenarios 2 and 3 (see Figures 5 and 7) are due to the topographical effects of the landscape surrounding the restoration areas. In Scenario 2, the steep hillsides on the left site of the river (see Figure 2b) are close to the river channel and act as flow barriers in the floodplains. The flow velocities are increased at this bottleneck, and the floodplain inundation changes downstream of the restoration intervention, which does not lead to the reconnection of floodplains. Neither the floodplain inundation frequencies nor the floodplain sedimentation increases. Therefore, it can be concluded that the location of the restoration strongly influences the success of the intervention.

River restoration interventions, such as removing fixed riverbeds and banks and initializing the dynamic and natural development of a river floodplain system, are not included in numerical model scenarios but lead to the reactivation of floodplains. For example, Straatsma and Kleinhans et al. (2018) numerically analyzed the effects of side channels, vegetation roughness smoothing, floodplain lowering, embankment relocation or lowering groynes, and minor embankments on the sediment transport in a river with embanked floodplains. Generally, the consequences of embankments due to the connectivity between floodplains and the riverbed are similar to those of a deeply incised river such as those analyzed in this study.

From an ecological point of view, fine sediments are often considered as negative and even substrates, which should be reduced or even removed from river-floodplain systems. For example, if the riverbed is predominantly (coarse) gravel, the fine sediment can deposit on or infiltrate the gravel riverbeds (Schruff, 2018). For stream managers, it is essential to estimate the potential damage due to fine sediment infiltration, such as the increased energy consumption of pumping wells, lower survival rates of fish spawn, or reduction of the hyporheic exchange of oxygen and nutrients (Schruff, 2018). In addition, contaminants might be adsorbed on fine-grained sediments (Brinkmann et al., 2015; Salomons et al., 1995; Schüttrumpf et al., 2011) and can therefore be deposited on the riverbed or floodplains and potentially be remobilized by subsequent flood events (Cofalla et al., 2012; Förstner, 2004; Zhao & Marriott, 2013).

River restoration interventions in old-industrial areas such as the ones analyzed in this study can have negative effects on the distribution of contaminants or positive effects because of the improvement of chemical and ecological conditions (Maaß et al., 2018). It is important to evaluate the contamination of a study site using its natural state because the initiation of natural morphodynamics includes the transport of fine sediment as an intrinsic component of river-floodplain systems. The deposition of fine sediments is a natural process that can only be increased by anthropogenic activity.

4.2. Historical and Present-Day Degree of Connectivity Between the Riverbed and the Floodplains

The analysis of the effects of river restorations, especially the effects of reactivated floodplains (in this study) on the fluvial morphodynamics, leads to the following questions: What does natural morphodynamics actually mean? Is a greater degree of connectivity between the river channel and floodplains really natural? What is the evidence for a greater degree of connectivity in the past?

Channel patterns describe the planform of a river, which reflects the interaction of the river channel with its floodplains and can change depending on environmental variations (Candel et al., 2018). Consequently, they reflect the degree of connectivity between the river channel and its floodplains. Candel et al. (2018) studied a low-energy valley river in the Netherlands and reported that the river was laterally stable from the Holocene to the Late Middle Ages and that meanders were anomalies. They found that the bankfull discharge was significantly greater during the meandering phase compared with the laterally stable phase (Candel et al., 2018). They also concluded that the change from the laterally stable to meandering phases might have occurred in other rivers for which an increased Holocene fluvial activity has been reported (Candel et al., 2018). With respect to the connectivity between the river channel and its floodplains, an increased bankfull discharge results in a decreased connectivity. Therefore, natural morphodynamics do not reflect a meandering river-floodplain system with a great degree of river-floodplain connectivity, as assumed in many river restoration interventions.

Recently, several studies focused on the anthropogenic history of the Wurm River and rivers like the Geul River or the Inde River with similar geomorphic settings, SSLs, and catchment sizes. The results of different studies by Buchty-Lemke and Lehmkuhl (2018), Hagemann et al. (2018), Maaß and Schüttrumpf (2018, 2019), and Maaß et al. (2018) show that floodplain sedimentation rates can be in an order of magnitude of 1 cm/year if the floodplains are prone to overbank flooding due to a constant impoundment of water at mill weirs and can be decreased to 0.1 cm/year due to incised riverbeds and riverbank heights of approximately 2 m. Here, the floodplain sedimentation rates of all numerical model scenarios vary between 0.5 and 1 cm/year that overall include natural as well as anthropogenic impacted floodplain accretion conditions of small river systems.

Focusing on the morphodynamic development, the results of these studies show that the Wurm River historically more dynamically meandered and that the floodplain sedimentation rates decreased. The anthropogenic impacts in terms of the construction and removal of water mills along the Wurm River led to the incision of the riverbed, disconnection of the riverbed from the floodplains, and increased bankfull discharge (Buchty-Lemke & Lehmkuhl, 2018; Maaß & Schüttrumpf, 2019). The comparison of the historical river course shown on Tranchot maps with the present-day river course indicated reductions in the river length, meanderin, and river gradient at a decreased sinuosity and meander migration rate (Buchty-Lemke and Lehmkuh, 2018).

With respect to the connectivity between the river channel and its floodplains, natural morphodynamics are based on a meandering river with a low bankfull discharge and consequently a high degree of connectivity, as assumed for many river restoration interventions. Consequently, it is important and indispensable to analyze and understand the past conditions of a river and define its natural conditions. The increase in the connectivity might not always lead to a natural morphological river state.

In this study, the numerical model results lead to the conclusion that only anthropogenic activity might have increased the amount of fine sediments deposited on floodplains and accelerated the process of floodplain decoupling from the riverbed in the past centuries. The reactivation of floodplains in river restorations, for example, by increasing the riverbed elevation or lowering the floodplains reduces, the anthropogenic floodplain sediment depositions and increases the degree of connectivity between the riverbed and floodplains. Within centuries to millennia, the connectivity between the floodplains and riverbed will decrease due to

the increasing floodplain elevation of floodplain sediment deposits. However, if a natural river state includes a larger degree of connectivity, the reactivation of floodplains will definitely increase the fluvial morphodynamics and lead to a natural, dynamic development of the river floodplain system. However, the deposition of fine sediments on floodplains and the ongoing potentially slow decoupling of floodplains from the riverbed are two intrinsic parts of natural river-floodplain systems and cannot be prevented in river restorations. Floodplain deposition is a natural process.

4.3. Assessment of the Model Quality and Assumptions

Model assumptions and schematizations are necessary and indispensable in nearly all numerical models and must be evaluated to determine their effects on the model quality (Straatsma & Kleinhans, 2018; Warmink et al., 2011). Berends et al. (2018) investigated the uncertainty of model predictions of intervention effects and analyzed its effects on the predictions of flood mitigation strategies. They concluded that model uncertainty does not invalidate model-supported decision making in river management but enriches it.

The effects of schematizing initial and boundary conditions and assumptions focusing on the suspended sediment transport on long-term numerical modeling studies have been extensively described by Maaß and Schüttrumpf (2018). In this study, numerical modeling scenarios are performed on only one sediment size fraction that is transported in suspension with a median diameter (D_{50}) of 24.5 μm (silt). The critical shear stress required for erosion of the floodplain was set to 12 N/m^2, and the maximum prevalent shear stress in the floodplains is only 8 N/m^2. Therefore, remobilization of floodplain deposits does not occur. If the sediment diameter of the model is smaller than 24.5 μm, resuspension of the particles might occur, and the sediment might not be deposited on the floodplains. If the sediment diameter of the model is larger than 24.5 μm, sediment deposition might occur closer to the channel, which would change the spatial distribution of the floodplain deposition. The numerical modeling scenarios in this study focus on long-term analysis, and short-term sediment transport processes, such as flocculation, resuspension, or coagulation, are not considered. Thus, the overall study results do not strongly depend on the chosen sediment diameter.

In this study, one of the main assumptions of the numerical modeling approach was that the river channel is fixed. As already summarized by Lauer and Parker (2008b), Wolman and Leopold (1957) stated that if vertical accretion on a floodplain continuously takes place without the removal of any sediment, the channel banks would grow in elevation until they eventually become too high such that the channel would rarely flood adjacent floodplains. In the long-term, this cause-effect relation would occur under the assumption of a fixed river channel. However, as meandering rivers migrate, they tend to remove material from cutbanks and deposit material in point bars and floodplains (Lauer & Parker, 2008b).

In natural river systems, local erosion phenomena and further incision of the riverbed occur over timescales of decades to centuries. These processes were not considered in the schematized numerical model, especially not in the different scenarios in this study, because the incision of the riverbed would lead to a disconnection of the floodplains from the riverbed. Neglecting these potential, locally developing erosion phenomena results in an overestimation of the reconnection of the floodplains, higher floodplain inundation rates, and higher fine sediment deposits on the floodplains.

The river bank erosion processes and river meandering were analyzed by Schuurman et al. (2016, 2018) using different numerical approaches. Schuurman et al. (2016) analyzed the interaction between bars and bends, which leads to meander initiation, and the effect of different methods on the modeled bank erosion and floodplain accretion dynamics of high-sinuosity channels with strong excitation when the inflow is periodically perturbed. Their study results show that both dynamic upstream inflow perturbation and bar-floodplain conversion are required for sustained high-sinuosity meandering (Schuurman et al., 2016). Schuurman et al. (2018) investigated the effects of higher peak discharges on the channel pattern and dynamics of bars, floodplain, and channel branches in a braided reach of the Upper Yellow River using a numerical model. Their results showed that the local-scale processes determining the channel-floodplain conversion and floodplain destruction have reach-scale effects on the braided river, and they indicated the need for physics-based methods for bank erosion modeling (Schuurman et al., 2018).

In addition to riverbank erosion and meandering, the effects of the cohesion of floodplain sediments and vegetation are also not considered in this study. Kleinhans et al. (2018) extensively compared the

isolated and combined effects of mud and vegetation on the river planform and morphodynamics in intermediate-size valley rivers using a numerical model for the century-scale simulation of the flow, sediment transport, and morphology. They concluded that valley-flooding water levels increase with the vegetation density, causing a higher braiding intensity rather than meandering tendency (Kleinhans et al., 2018). They also concluded that an increase in the concentration of floodplain aggradation reduces the overbank flow frequency and ultimately causes the formation of single-thread channels (Kleinhans et al., 2018).

Considering such natural morphodynamic processes, such as meander migration, changes in the river course, and river widening or narrowing, in a numerical model is only possible by making further assumptions and schematizations (Spruyt et al., 2011) and not applicable for numerical models with timescales of decades to centuries. Overall, the impact of natural processes and human activities on a catchment area increases with decreasing catchment size, and not all impact factors can be implemented in detail in a numerical model. The schematization, discretization, and parameterization are indispensable regarding the grid approximation, course of the river, water inflow, and sediment input as well as erosion and deposition processes especially for long-term morphological modeling investigations. However, the numerical model results are always a useful tool to assess river management strategies. Based on a schematized river-floodplain system representing the main characteristics of a set of systems (here small gravel bed rivers deeply incised with large amounts of fine sediment deposited on the floodplains), the consequences of different scenarios can be investigated in an appropriate period, and the fundamental changes of fine sediment deposits on floodplains can be determined.

5. Conclusions

In addition to many other measures, increasing the riverbed elevation or lowering the floodplain elevation are two examples of river restoration interventions focusing on an increase of the surface water connectivity between the main channel of a river and its floodplains. Such a reactivation potentially has extensive consequences on the fluvial morphodynamics and mobility of fine sediments. The objective of this study was to analyze the long-term effects of reactivated floodplains on the mobility of floodplain deposits of small rivers. The long-term changes of the floodplain sedimentation rates were determined using a numerical model based on the Delft3D software. The characteristics of the numerical model were based on the characteristics of the Wurm River (Lower Rhine Embayment, Germany) as an example for a small meandering lowland river in Western Europe impacted by diverse natural and anthropogenic factors. The results of the model scenarios show the following:

- The increase in the riverbed elevation and lowering of the floodplains generally lead to higher-floodplain sedimentation rates.
- Lowering the floodplains has a greater impact on the reactivation of floodplains than the increase in the riverbed elevation independent of the location of the restoration area, because floodplain inundation occurs earlier during the discharge, which leads to longer sediment settling.
- The increase in the surface water connectivity of an elevated riverbed with its floodplains strongly depends on the location and topography of the restoration area considering also depletion of sediment in downstream direction if the restoration is located in an upstream part of the river.
- River restorations can lead to increased flow velocities and alter the floodplain connectivity downstream of the restoration intervention, leading to floodplain inundation at earlier discharge stages and longer sediment settling.

Overall, based on the assumption of a fixed river channel, the reactivation of floodplains in river restorations decreases because anthropogenic activity accelerates floodplain sediment deposition and leads to a greater degree of connectivity between the riverbed and floodplains. In this study, this process is predominantly driven by the increase in floodplain inundation at earlier discharges due to lowering of floodplains. However, such a reactivation of floodplains will increase the fluvial morphodynamics and lead to a natural, dynamic development of the river floodplain system, but the deposition of fine sediments on floodplains and ongoing, potentially slow decoupling of floodplains from the riverbed are two intrinsic parts of natural river-floodplain systems and cannot be prevented by river restorations.

Acknowledgments

This study is part of the research in the project "Human impact on fluvial morphodynamics and contaminant dispersion in small river catchments (case study: Wurm, Lower Rhine Embayment)" funded by the German Research Foundation (Deutsche Forschungsgemeinschaft, Grant FR3509/3-1). We sincerely acknowledge R. M. Frings for his effort and advice in the development of this paper. The cross-sectional profiles of the Wurm River were generously provided by Bezirksregierung Köln, Dezernat 54, Wasserwirtschaft and are not freely accessible due to a user agreement. The discharge and water level data sets were kindly provided by Landesamt für Natur, Umwelt und Verbraucherschutz Nordrhein-Westfalen (LANUV). For the Digital Elevation Model (DEM) see Land NRW (2017). Datenlizenz Deutschland—Digitales Geländemodell Gitterweite 1 m—Version 2.0 (https://www.govdata.de/dl-de/by-2-0). For the discharges and water levels measured in the Wurm River see LANUV (2018). Datenlizenz Deutschland—Wasserstände und Abflüsse im Einzugsgebiet der Wurm in 5 min Abständen—Version 2.0 (https://www.govdata.de/dl-de/by-2-0). The raw data of the turbidity and SSC measurements are uploaded in a data repository (10.6084/m9.figshare.9784328). We sincerely thank T. Schruff and J. Oetjen for the technical discussions and writing suggestions. We also thank the reviewers whose comments significantly improved the original manuscript.

References

Asselman, N. E. M., & Middelkoop, H. (1995). Floodplain sedimentation: Quantities, patterns and processes. *Earth Surf. Process. Landforms*, *20*, 481–499. https://doi.org/10.1002/esp.3290200602

Berends, K. D., Straatsma, M. W., Warmink, J. J., & Hulscher, S. J. M. H. (2018). Uncertainty quantification of flood mitigation predictions and implications for decision making. *Natural Hazards and Earth System Sciences*, 1–25. https://doi.org/10.5194/nhess-2018-325

Bizzi, S., Dinh, Q., Bernardi, D., Denaro, S., Schippa, L., & Soncini-Sessa, R. (2015). On the control of riverbed incision induced by run-of-river power plant. *Water Resources Research*, *51*, 5023–5040. https://doi.org/10.1002/2014WR016237

Brinkmann, M., Eichbaum, K., Reininghaus, M., Koglin, S., Kammann, U., Baumann, L., et al. (2015). Towards science-based sediment quality standards—Effects of field-collected sediments in rainbow trout (Oncorhynchus mykiss). *Aquatic Toxicology*, 50–62.

Brunotte, E., Dister, E., Günther-Diringer, D., Koenzen, U., & Mehl, D. (2009). *Flussauen in Deutschland*. Erfassung und Bewertung des Auenzustandes. Naturschutz und biologische Vielfalt.

Buchanan, P. A., & Schoellhamer, D. H. (1995). *Summary of suspended-solids concentration data, Central and South San Francisco Bays*. California: Water years 1992 and 1993.

Buchty-Lemke, M., & Lehmkuhl, F. (2018). Impact of abandoned water mills on Central European foothills to lowland rivers: A reach scale example from the Wurm River. Germany, Geografiska Annaler: Series A. *Physical Geography*, *10*, 1–19. https://doi.org/10.1080/04353676.2018.1425621

Candel, J. H. J., Kleinhans, M. G., Makaske, B., Hoek, W. Z., Quik, C., & Wallinga, J. (2018). Late Holocene channel pattern change from laterally stable to meandering—A palaeohydrological reconstruction. *Earth Surf. Dynam.*, *6*, 723–741. https://doi.org/10.5194/esurf-6-723-2018

Christensen, V. G., Jian, X., & Ziegler, A. C. (2000). Regression analysis and real-time water quality monitoring to estimate constituent concentrations, loads, and yields in the Little Arkansas River. *South-Central Kansas*, 1995–1999.

Cofalla, C., Hudjetz, S., Roger, S., Brinkmann, M., Frings, R., Wölz, J., et al. (2012). A combined hydraulic and toxicological approach to assess re-suspended sediments during simulated flood events—Part II: An interdisciplinary experimental methodology. *J Soils Sediments*, *12*, 429–442. https://doi.org/10.1007/s11368-012-0476-2

Davies-Colley, R. J., & Smith, D. G. (2001). Turbidity suspended sediment and water clarity: A review. *Journal of American Resources Association*, *37*, 1085–1101. https://doi.org/10.1111/j.1752-1688.2001.tb03624.x

Ehlert, T., & Neukirchen, B. (2012). *Zustand und Schutz der Flussauen in Deutschland*. Natur und Landschaft, 4, 161–167, Kohlhammer Stuttgart

Fassoni-Andrade, A. C., & Dias de Paiva, R. C. (2019). Mapping spatial-temporal sediment dynamics of river-floodplains in the Amazon. *Remote Sensing of Environment*, *221*, 94–107. https://doi.org/10.1016/j.rse.2018.10.038

Fischer, R. (2000). Einzugsgebiet Maas. Entwicklung der Gewässergüte in der Wurm. In: LANUV NRW (ed), Gewässergüte.

Förstner, U. (2004). Sediment dynamics and pollutant mobility in rivers: An interdisciplinary approach. *Lakes Reserv Res Manage*, *9*, 25–40. https://doi.org/10.1111/j.1440-1770.2004.00231.x

Frings, R. M., Berbee, B. M., Erkens, G., Kleinhans, M. G., & Gouw, M. J. P. (2009). Human-induced changes in bed shear stress and bed grain size in the River Waal (The Netherlands) during the past 900 years. *Earth Surface Processes and Landforms*, *34*, 503–514. https://doi.org/10.1002/esp.1746

Ghoshal, S., James, L. A., Singer, M. B., & Aalto, R. (2010). Channel and floodplain change analysis over a 100-year period: Lower Yuba River. *California, Remote Sensing*, *2*, 1797–1825. https://doi.org/10.3390/rs2071797

Gilvear, D. J., & Petts, G. E. (1985). Turbidity and suspended solids variations downstream of a regulating reservoir. *Earth surface processes and landforms*, *10*, 363–373. https://doi.org/10.1002/esp.3290100408

Gippel, C. J. (1989). The use of turbidimeters in suspended sediment research. *Hydrobiologia*, *176-177*, 465–480. https://doi.org/10.1007/BF00026582

Gippel, C. J. (1995). Potential of turbidity monitoring for measuring the transport of suspended solids in streams. *Hydrological Processes*, *9*, 83–97. https://doi.org/10.1002/hyp.3360090108

Habersack, H., Haimann, M., Kerschbaumsteiner, W., & Lalk, P. (2008). *Schwebstoffe in Fließgewässern*. Leitfaden zur Erfassung des Schwebstofftransportes, AV+Astoria Druckzentrum: Wien.

Hagemann, L., Buchty-Lemke, M., Lehmkuhl, F., Alzer, J., Kümmerle, E. A., & Schwarzbauer, J. (2018). Exhaustive screening of long-term pollutants in riverbank sediments of the Wurm River, Germany. *Water Air Soil Pollut*, *229*, 290. https://doi.org/10.1007/s11270-018-3843-9

Hoffmann, T., Hillebrand, G., Schmegg, J., & Volmer, S. (2017). Monitoring long-term suspended sediment yields in Germany: Quality controls on changing sediment sampling strategies. *In: HydroSenSoft (ed)*. International Symposium and: Exhibition on Hydro-Environment Sensors and Software.

Kern, K. (1998). *Sohlenerosion und Auenauflandung: Empfehlungen zur Gewässerunterhaltung*. Broschüre, Gemeinnützige Fortbildungsgesellschaft für Wasserwirtschaft und Landschaftsentwicklung: Mainz.

Kleinhans, M.G., de Vries, B., Braat, L., & van Oorschot, M. (2018). Living landscapes: Muddy and vegetated floodplain effects on fluvial pattern in an incised river. *Earth Surf. Process. Landforms 43*:2948–2963. https://doi.org/10.1002/esp.4437

Lambert, C. P., & Walling, D. E. (1987). Floodplain sedimentation: A preliminary investigation of contemporary deposition within the lower reaches of the River Culm, Devon, UK. *Geografiska Annaler: Series A, Physical Geography*, *69*, 393–404. https://doi.org/10.1080/04353676.1987.11880227

Land NRW (2017). Datenlizenz Deutschland—Digitales Geländemodell Gitterweite 1 m—Version 2.0 (https://www.govdata.de/dl-de/by-2-0).

LANUV NRW (2004). Ergebnisbericht Rur und südliche sonstige Maaszuflüsse. Bearbeitungsgebiet Maas-Deutschland (Süd). In *Wasserrahmenrichtlinie in NRW – Bestandsaufnahme*, Ministerium für Umwelt und Naturschutz, Landwirtschaft und Verbraucherschutz des Landes Nordrhein-Westfalen: Düsseldorf.

LANUV NRW (2018). Datenlizenz Deutschland—Wasserstände und Abflüsse im Einzugsgebiet der Wurm in 5 min Abständen—Version 2.0 (https://www.govdata.de/dl-de/by-2-0).

Lauer, J. W., & Parker, G. (2008a). Modeling framework for sediment deposition, storage, and evacuation in the floodplain of a meandering river: Application to the Clark Fork River. *Montana. Water Resour. Res.*, *44*, 179. https://doi.org/10.1029/2006WR005529

Lauer, J. W., & Parker, G. (2008b). Net local removal of floodplain sediment by river meander migration. *Geomorphology*, *96*, 123–149. https://doi.org/10.1016/j.geomorph.2007.08.003

Lesser, G. R. (2009). *An approach to medium-term coastal morphological modelling*. Leiden: CRC Press/Balkema.

Lesser, G. R., Roelvink, J. A., van Kester, J. A. T. M., & Stelling, G. S. (2004). Development and validation of a three-dimensional morphological model. *Coastal Engineering*, *51*, 883–915. https://doi.org/10.1016/j.coastaleng.2004.07.014

Lewis, J. (1996). Turbidity-controlled suspended sediment sampling for runoff-event load estimation. *Water Resources Research*, *32*, 2299–2310. https://doi.org/10.1029/96WR00991

Lietz, A. C., & Debiak, E. A. (2005). *Development of rating curve estimators for suspended-sediment concentration and transport in the C-51 canal based on surrogate technology*, (pp. 2004–2005). Florida: Plam Beach County.

Maaß, A.-L., Esser, V., Frings, R. M., Lehmkuhl, F., & Schüttrumpf, H. (2018). A decade of fluvial morphodynamics: Relocation and restoration of the Inde River (North-Rhine Westphalia, Germany). *Environmental Sciences Europe.*. https://doi.org/10.1186/s12302-018-0170-0

Maaß, A.-L., & Schüttrumpf, H. (2018). Long-term effects of mining-induced subsidence on the trapping efficiency of floodplains. *Anthropocene*, *24*, 1–13. https://doi.org/10.1016/j.ancene.2018.10.001

Maaß, A.-L., & Schüttrumpf, H. (2019). *Elevated floodplains and net channel incision as a result of the construction and removal of water mills*. Geografiska Annaler: Series A, Physical Geography. https://doi.org/10.1080/04353676.2019.1574209

Marquis, P. (2005). *Turbidity and suspended sediment as measures of water quality*. Watershed Management Bulleting: Streamline.

Middelkoop, H., & van der Perk, M. (1998). Modelling spatial patterns of overbank sedimentation on embanked floodplains. Geografiska Annaler: Series A. *Physical Geography*, *80*, 95–109.

MULNV NRW (2008). Mehr Lebenfür die Wurm und den Senserbach. Der Fluss, die Bäche und das Grundwasser im Gebiet der Wurm und des Senserbaches. In *Zustand*. Düsseldorf: Ursachen von Belastungen und Maßnahmen, 1-39.

Narinesingh, P., Klaassen, G. J., & Ludikhuize, D. (2010). Floodplain sedimentation along extended river reaches. *Journal of Hydraulic Research*, *37*, 827–845. https://doi.org/10.1080/00221689909498514

Nash, J. E., & Sutcliffe, J. V. (1970). River flow forecasting through conceptual models part I—A discussion of principles. *Journal of Hydrology*, *10*, 282–290. https://doi.org/10.1016/0022-1694(70)90255-6

Partheniades, E. (1965). Erosion and deposition of cohesive soils. *ASCE Journal of Hydraulic Division*, 105–139.

Rasmussen, T. J., Ziegler, A. C., & Rasmussen, P. P. (2005). Estimation of constituent concentrations. *densities, loads and yields on lower Kansas River, Northeast Kansas, using regression models and continuous water-quality modeling. January 2000 through*, (December 2005).

Rudorff, C. M., Dunne, T., & Melack, J. M. (2018). Recent increase of river-floodplain suspended sediment exchange in a reach of the lower Amazon River. *Earth Surf. Process. Landforms*, *43*, 322–332. https://doi.org/10.1002/esp.4247

Salomons, W., Förstner, U., & Mader, P. (1995). *Heavy metals*. Problems and solutions, Springer: Berlin, Heidelberg.

Scheffers, A. M., May, S. M., & Kelletat, D. H. (2015). Landforms of the world with Google Earth: Understanding our environment. In *Springer Netherlands, Imprint*. Dordrecht: Springer, 1-391.

Schoelhammer, D. H., & Scott, A. W. (2003). Continuous measurement of suspended-sediment discharge in rivers by use of optical backscattering. In J. Bogen, T. Fergus, & E. Walling (Eds.), *Erosion and sediment transport measurement in rivers: Technological and methodological advances: Papers selected from the workshop ... held in Oslo, Norway, 19-21 june 2002*. Wallingford: IAHS Press.

Schruff, T. (2018). *Taking a closer look at the causes and impacts of fine sediment infiltration into gravel beds: Development and application of an extended theory of fine sediment infiltration based on grain scale numerical simulations*. Dissertation: RWTH Aachen University.

Schüttrumpf, H., Brinkmann, M., Cofalla, C., Frings, R. M., Gerbersdorf, S. U., Hecker, M., et al. (2011). A new approach to investigate the interactions between sediment transport and ecotoxicological processes during flood events. *Environ Sci Eur*, *23*(39). https://doi.org/10.1186/2190-4715-23-39

Schuurman, F., Shimizu, Y., Iwasaki, T., & Kleinhans, M. G. (2016). Dynamic meandering in response to upstream perturbations and floodplain formation. *Geomorphology*, *253*, 94–109. https://doi.org/10.1016/j.geomorph.2015.05.039

Schuurman, F., Ta, W., Post, S., Sokolewicz, M., Busnelli, M., & Kleinhans, M. G. (2018). Response of braiding channel morphodynamics to peak discharge changes in the Upper Yellow River. *Earth Surf. Process. Landforms*, *43*, 1648–1662. https://doi.org/10.1002/esp.4344

Spruyt, A., Mosselman, E., & Jagers, B. (2011). *A new approach to river bank retreat and advance in 2D numerical models of fluvial morphodynamics, River, Coastal and Estuarine Morphodynamics*. Beijing: RCEM2011, Tsinghua University Press.

Straatsma, M. W., & Kleinhans, M. G. (2018). Flood hazard reduction from automatically applied landscaping measures in RiverScape, a Python package coupled to a two-dimensional flow model. *Environmental Modelling & Software*, *101*, 102–116. https://doi.org/10.1016/j.envsoft.2017.12.010

Surian, N., & Rinaldi, M. (2003). Morphological response to river engineering and management in alluvial channels in Italy. *Geomorphology*, *50*, 307–326. https://doi.org/10.1016/S0169-555X(02)00219-2

Surian, N., Ziliani, L., Comiti, F., Lenzi, M. A., & Mao, L. (2009). Channel adjustments and alteration of sediment fluxes in gravel-bed rivers of North-Eastern Italy: Potentials and limitations for channel recovery. *River Research and Applications*, *25*, 551–567. https://doi.org/10.1002/rra.1231

Uhrich, M. A., & Bragg, H. M. (2003). Monitoring in-stream turbidity to estimate continuous suspended-sediment loads and yields and clay-water volumes in the Upper North Santiam River Basin. *Oregon*, 1998–2000.

van Denderen, R. P., Schielen, R. M. J., Blom, A., Hulscher, S. J. M. H., & Kleinhans, M. G. (2018). Morphodynamic assessment of side channel systems using a simple one-dimensional bifurcation model and a comparison with aerial images. Earth Surf. Process. *Landforms*, *43*, 1169–1182. https://doi.org/10.1002/esp.4267

Vogt, H. (1998). *Niederrheinischer Wassermühlenführer*. Krefeld: Verein Niederrhein.

Walling, D. E. (1977). Assessing the accuracy of suspended sediment rating curves for a small basin. *Water Resources Research*, *13*, 531–538. https://doi.org/10.1029/WR013i003p00531

Warmink, J. J., van der Klis, H., Booij, M. J., & Hulscher, S. J. M. H. (2011). Identification and quantification of uncertainties in a hydrodynamic river model using expert opinions. *Water Resources Management*, *25*, 601–622. https://doi.org/10.1007/s11269-010-9716-7

Wohl, E., Lane, S. N., & Wilcox, A. C. (2015). The science and practice of river restoration. *Water Resources Research*, *51*, 5974–5997. https://doi.org/10.1002/2014WR016874

Wolman, M. G., & Leopold, L. B. (1957). *River flood plains: Some observations on their formation*. Washington, DC: U.S. Geological Survey Professional Paper vol. 282-C.

Yossef, M. F. M., Jagers, H. R. A., Vuren, S. V., & Sieben, A. (2008). Innovative techniques in modelling large-scale river morphology. In M. Altinakar (Ed.), *Proceedings of the International Conference on Fluvial Hydraulics: River flow 2008*, 3-13. Izmir, Turkey, Kubaba Congress Department and Travel Services, Ankara: Cesme.

Zhao, Y., & Marriott, S. B. (2013). Dispersion and remobilisation of heavy metals in the River Severn System, UK. *Procedia Environmental Sciences*, *18*, 167–173. https://doi.org/10.1016/j.proenv.2013.04.022